International Journal of Biological Macromolecules 163 (2020) 865–877

Contents lists available at ScienceDirect

International Journal of Biological Macromolecules

journal homepage: http://www.elsevier.com/locate/ijbiomac

Characterization of a polysaccharide from *Sanghuangporus vaninii* and its antitumor regulation via activation of the p53 signaling pathway in breast cancer MCF-7 cells

Xilin Wan [a,b], Xin Jin [c], Mengle Xie [c], Jie Liu [d], Andrey A. Gontcharov [e], Huan Wang [b], Ruina Lv [a], Daiyao Liu [a], Qi Wang [a,*], Yu Li [a,*]

[a] Engineering Research Center of Edible and Medicinal Fungi, Ministry of Education, Jilin Agricultural University, Changchun 130118, China
[b] Jilin Ginseng Academy, Changchun University of Chinese Medicine, Changchun 130117, China
[c] Key Laboratory of Molecular Epigenetics of the Ministry of Education (MOE), Northeast Normal University, Changchun 130024, China
[d] Yanbian Xinglin Biotechnology Co., Ltd, Helong 133500, China
[e] Institute of Biology and Soil Science FEB RAS, 100-letia Vladivostoka prospect, 159, Vladivostok 690022, Russia

ARTICLE INFO

Article history:
Received 26 April 2020
Received in revised form 24 June 2020
Accepted 29 June 2020
Available online 03 July 2020

Keywords:
Sanghuangporus vaninii
Polysaccharide
Characterization
Antitumor activity
Breast cancer
MCF-7 cells

ABSTRACT

Sanghuangporus is a traditional medicine that has been used for nearly 2000 years in Asia. It has been found to enhance immunity and have anticancer properties. Some studies determined that *Sanghuangporus* polysaccharide can inhibit tumors in vitro, although the underlying mechanisms remain unknown. Therefore, the present study investigated the antitumor effects of polysaccharides from the fruiting body of *S. vaninii* and their associated mechanisms. Water-soluble *S. vaninii* polysaccharide (SVP) with a molecular weight of 3.156×10^4 Da was isolated and found to be mainly composed of mannose, rhamnose, glucuronic acid, galacturonic acid, glucosamine, glucose, galactosamine, galactose, xylose, arabinose, and fucose in molar ratios of 1.63:0.04:0.36:0.03:0.13:8.39:0.08:1.08:0.25:1.07:0.40. SVP showed modest anti-proliferative activity against HeLa, SHG-44, SMMC-7721, and MCF-7 cells. Furthermore, it effectively regulated cell cycle, promoted apoptosis, and reduced the migratory and invasive capacities of MCF-7 cells. Mechanistically, SVP enhanced activation of p53-related genes and down-regulated MMP expression. These findings describe a potential natural polysaccharide for tumor therapy and a basis for the development of fungal polysaccharides as a type of health food.

1. Introduction

Breast cancer is the second leading cause of death among all cancers, and mostly occurs in women [1]. In recent years, it has been found that polysaccharides have a wide range of biological activities, such as antitumor [2], enhanced immunity [3], antimicrobial, and antioxidant [4] activities. Most of these can inhibit tumor cell proliferation, promote cell apoptosis, inhibit tumor cell migration, or activate macrophages to improve the body's immune response to tumor cells in order to achieve the antitumor effect of polysaccharide components.

Fungal polysaccharides have also shown some promise [5]. Lentinan is the most widely studied fungal polysaccharide [6–9]. Currently, it has been used clinically in many Asian countries, especially China, Japan, and South Korea. *Cordyceps sinensis* polysaccharide can induce apoptosis and autophagy flux blockage in colon cancer cells [10]. *Flammulina velutipes* polysaccharide can significantly enhance natural killer cell activity against K562 tumor cells in vitro [11]. However, fungi such as *Lentinula edodes*, *Cordyceps sinensis,* and *Flammulina velutipes*, which have excellent biological activity, all belong to the edible fungus and functional food groups. Some wood fungi cannot serve as food yet have good pharmacological effects. These include *Phellinus linteus* [12], *Phellinus igniarius* [13], *Inonotus obliquus* [14], and *Ganoderma lucidum* [15]. Therefore, fungus polysaccharides have potential value in clinical applications and product development.

Sanghuangporus [16] is as a traditional medicine that can be traced back 2000 years in China. “Sanghuang” has been used as a traditional Chinese medicine for the treatment of diarrhea, night sweats, metrorrhagia, drench, stomach pain, prolapse of spilled blood, leucorrhea, and amenorrhoea. However, “Sanghuang” in traditional Chinese medicine differs from “*Sanghuangporus*” in current taxonomy. *Sanghuangporus vaninii* has the largest market share in traditional Chinese medicine, while *Sanghuangporus baumii* has the second largest. Although many people think that wild *Sanghuangporus sanghuang* has excellent biological activity, the lack of accurate strain identification and artificial cultivation of *Sanghuangporus sanghuang* also presents technical difficulties.

* Corresponding authors at: No. 2888 Xincheng Street, Jilin Agricultural University, Changchun 130118, China.
E-mail addresses: qiwang@jlau.edu.cn (Q. Wang), yuli966@126.com (Y. Li).

https://doi.org/10.1016/j.ijbiomac.2020.06.279
0141-8130/

Both Japanese and Korean mycologists have adopted *P. linteus* as a scientific name for "Sanghuang" more than half a century ago [17]. *Sanghuangporus* was established as a new genus in 2016, with 14 species to date [18]. The main active components of *Sanghuangporus* include polysaccharides [19], phenols [20], flavonoids [21], coumarins [22], terpenoid [23], furan [24], and others [25–29]. However, it is difficult to find the fruiting body of *S. sanghuang* in the wild for picking.

Most previous studies have focused on the cultivation of *Sanghuangporus*, extraction, isolation, and component identification. There are relatively few studies on the mechanism of action of its active components [12]. In China, scientists have achieved artificial domestication and cultivation of wild *S. vaninii* through bagged and cut-log cultivation. However, little is known about the effect of *S. vaninii*. Therefore, this study focused on the polysaccharide component of *S. vaninii* in order to explore whether artificially cultivated *S. vaninii* has disease-resisting properties and to provide a theoretical basis for its development as medicine and functional food.

In this study, the fungal species were identified and polysaccharide components were extracted. Further, the anti-tumor bioactivity and mechanisms of SVP were explored to identify important molecular targets in cancer progression.

2. Materials and methods

2.1. Materials and reagents

Samples were randomly collected from the cultivation greenhouse of Yanbian Xinglin Biotechnology Co., Ltd. All samples were cultivated for three years from 2016 to 2019. All antibodies were purchased from ABclonal (Wuhan, China). DEAE-cellulose DE-52 (S14024) and Sephadex G200 (S14036) were purchased from Shanghai yuanye Bio-Technology Co., Ltd. Other chemicals and reagents were of analytical grade and supplied by Sigma-Aldrich.

2.2. Species identification

The samples were dried naturally for one month, and then crushed into powder and passed through the sieve. Fungal DNA was extracted from the samples using the Ezup Column Fungi Genomic DNA Purification Kit (NO. B518259, Sangon Biotech). Then, PCR was performed to amplify the genome. The ITS sequence primers were as follows: ITS1: TCCGTAGGTGAACCTGCGG, ITS4: TCCTCCGCTTATTGATATGC. Product length was 600 bp. Reaction conditions were as follows: 94 °C (4 min), 94 °C (45 s) → 55 °C (45 s) → 72 °C (1 min) for 30 cycles, 72 °C (10 min), 1% agarose electrophoresis, 150 V, 100 mA, with 20 min for electrophoresis observation.

PCR products were directly sequenced by PCR primers. The purification was performed according to the instructions provided in the San Prep Column DNA Gel Extraction Kit (B518131, Sangon Biotech). The sequencing results were obtained from BLAST in the National Center of Biotechnology Information (NCBI) to determine the strain.

2.3. SVP preparation

2.3.1. SVP extraction

The crushed sample powder was soaked in 95% ethanol for 24 h to remove fat and repeated three times. Ethanol was then recovered and the remaining extract was reserved for further use. The solid sample (100 g) was extracted with distilled water (30 L). The sample was boiled in water and concentrated using a rotary evaporator. Ethanol was added to the sample so that the volume of ethanol accounted for 80% of the total volume. The polysaccharide components were then extracted and lyophilized samples were ready for further purification.

2.3.2. SVP purification

The extracted SVP precipitate was re-dissolved in deionized water. The sample was purified using a DEAE-cellulose DE-52 column (3 cm × 75 cm) eluted with distilled water and 0.1 M NaCl at 1 mL/min with 10 mL/tube. The sodium chloride elution samples were then dialyzed, desalted, and lyophilized. Finally, the mixture was purified using a Sephadex G-200 column (3 cm × 60 cm) eluted with distilled water at 1 mL/min. The sample was then lyophilized for further research.

2.4. SVP characteristics

2.4.1. Molecular weight and component determination

The molecular weight of the polysaccharides was determined using the Gel Permeation Chromatography (GPC) method, Wyatt Sec-Mals with Dawn Heleos - II laser detector, Optilab rex refractive index detector, Shodex OHpak SB-806 HQ chromatographic column, 0.1 M sodium sulfate, and 0.2% sodium azide in a mobile phase at 0.5 mL/min. The sample concentration was 2 mg/mL in 500 μL of solution. The running time was 35 min with glucan 40,000 reference substance normalized processing. The absolute molecular weight was calculated using the principle of light scattering.

Ultraviolet spectrophotometer was used to detect nucleic acid and protein contamination via absorbance scanning between 200 and 600 nm.

2.4.2. FT-IR determination

A Fourier transform infrared spectrometer (FT-IR) detected the absorption spectrum and determined the composition of the samples. The wave number was scanned in the range of 4000–400 cm^{-1} to test the transmittance of the sample.

2.4.3. Monosaccharide composition

Monosaccharide composition was tested using high-performance liquid chromatography (HPLC, Thermo Scientific Dionex Ulti Mate 3000 Series). The standard monosaccharide composition included mannose, rhamnose, glucuronic acid, galacturonic acid, glucosamine, glucose, galactosamine, galactose, xylose, arabinose, and fucose. Trifluoroacetic acid was used to hydrolyze the SVP. Then, sodium hydroxide and PMP-methyl alcohol were added into the sample to derivate at 30 °C for 1 h. Hydrochloric acid and chloroform were then added and the solution maintained at 3000 r/min for 10 min. The supernatant was extracted three times. The detection conditions were as follows: column temperature was 30 °C, flow velocity was 0.1 mL/min, injection volume was 40 μL, mobile phase was potassium dihydrogen phosphate solution, and detection wavelength was set at 250 nm.

2.5. Cell lines and cell culture

All of the cell lines were obtained from Shanghai Cell Bank, Chinese Academy of Sciences. Cervical carcinoma HeLa, glioma SHG-44, and hepatocellular carcinoma SMMC-7721 cells were cultured in DMEM with 10% newborn calf serum. Human breast cancer cells MCF-7 were cultured in special medium (CM-0149, Procell Life Science & Technology Co., Ltd.). All media contained 100 μg/mL of streptomycin and 100 units/mL of penicillin G.

2.6. Cell proliferation assay

Cell Counting Kit-8 (CCK-8, MCE, HY-K0301) utilizes highly water-soluble tetrazolium salt. WST-8 [2-(2-methoxy-4-nitrophenyl)-3-(4-nitrophenyl)-5-(2,4-disulfophenyl)-2H-tetrazolium, monosodium salt] produces a water-soluble formazan dye upon reduction in the presence of an electron mediator. CCK-8 is therefore a sensitive colorimetric assay used for the determination of the number of viable cells during cell proliferation and as a cytotoxicity test.

MCF-7 cells (6×10^3/well) were cultured in each well of the 96-well plate. Cells were cultured for 24 h and medium was replaced with medicated medium containing 0–800 μg/mL of SVP. Doxorubicin hydrochloride was selected as a positive control drug due to its extensive antitumor effects. Doxorubicin hydrochloride inhibited topoisomerase II, thereby inhibiting DNA replication. It promoted apoptosis and autophagy and inhibited human DNA topoisomerase I. Its IC_{50} was 0.8 μM. The dosage was set at 2 μM.

Each concentration was tested five times and at least three parallel tests were conducted according to the following instructions: the CCK-8 dosage was added to the medium at a ratio of 1:10 and the cells were incubated at 37 °C for 30 min. The absorbance at 450 nm was then measured using a microplate reader. The absorbance value with and without SVP treatment was measured and inhibition rate was calculated using the following formula:

$$\text{Inhibition rate}\ (\%) = \left(\left[A_{\text{without drugs}} - A_{\text{with drugs}}\right] / \left[A_{\text{without drugs}} - A_{\text{blank control}}\right]\right) \times 100\%$$

2.7. Cell cycle and apoptosis analysis

MCF-7 cells (4×10^5/well) were cultured in six-well plates for 24 h and follow-up experiments were conducted in accordance with the instructions supplied with the Cell Cycle and Apoptosis Analysis Kit (Beyotime, China). At least three parallel tests were conducted.

2.8. Colony formation assay

MCF-7 cells (3×10^2/well) were cultured for 24 h in six-well plates with MEM medium. Then, the medium was replaced with medicated medium containing 0–800 μg/mL of SVP. The fresh medium was changed every three days and cultured continuously for 21 days. The number of cell clones was counted under the microscope after crystal violet staining. Culture images were also obtained. The experiment was repeated three times at each concentration.

2.9. Cell apoptosis analysis

MCF-7 cells (4×10^5/well) were cultured in six-well plates for 24 h and medium was replaced with medicated medium containing 0–800 μg/mL of SVP. Follow-up experiments were conducted in accordance with the instructions supplied with the Annexin V - FITC and PI cell Apoptosis Analysis Kits (KeyGENE BioTECH, China). Three parallel tests were conducted.

2.10. Scratch wound healing assay

MCF-7 cells (6×10^5/well) were cultured for 24 h. When cell coverage reached 85%, a pipette tip was used to scratch the cell surface. Medium was then replaced with fresh medium containing SVP (0–800 μg/mL). Images were taken under a microscope at 0, 24, and 48 h. Fixed positions were marked on the images in order to obtain photographs of the same areas for each time point. Cell migration coverage rate within the scratch was calculated. Three parallel tests were conducted.

2.11. Migration and invasion analysis

MCF-7 cells (1×10^5/well) were added into the cell migration chamber in 24-well plates. Medium containing SVP at different concentrations (0–800 μg/mL) was used. After a 24-h culture, crystal violet-stained cells crossed the membrane and their images were obtained for quantification under a constant light microscope. Six pictures were taken for each sample. The experiment was repeated at least three times at each concentration.

2.12. Quantitative real-time polymerase chain reaction (qPCR)

Total RNA was extracted from each sample and used to prepare cDNA samples to measure gene expression by qPCR with primers presented in Table 1. Reaction conditions were as follows: 95 °C (5 min), 95 °C (30 s) → 55 °C (45 s) → 72 °C (30 s) for 40 cycles, 72 °C for 10 min.

2.13. Western blotting

Cells were collected and analyzed with radioimmunoprecipitation assay (RIPA) buffer for Western blot analysis. Protein samples (50–100 μg) were separated using 12% dodecyl sulfate, sodium salt (SDS)-polyacrylamide gel electrophoresis (SDS-PAGE), transferred to a polyvinylidene fluoride (PVDF) membrane for 3 h, and blocked with 5% bovine serum albumin (BSA) in Tris-buffered saline-Tween (TBST) for 1 h. Primary antibodies anti-β-actin (AC038, ABclonal), anti-Bax (A19684, ABclonal), anti-Bcl-2 (A19693, ABclonal), anti-p53 (A3185, ABclonal), anti-MMP-2 (A19080, ABclonal), anti-MMP-9 (A11147, ABclonal), anti-caspase-3 (A19654, ABclonal), anti-caspase-9 (A0281, ABclonal), anti-caspase-8 (A11324, ABclonal), anti-PARP (A19596, ABclonal), and anti-P21 (A1483, ABclonal) were incubated for 2 h at room temperature (1:1000). The membranes were then washed three times, probed with secondary antibodies, and an ECL kit was used for visualization with a Tanon-5200 imaging system (Tanon, China).

2.14. Statistical analysis

All data were expressed as mean ± standard error of the mean (SEM). Each experiment included at least three replicates and all data were analyzed using Microsoft Excel and SPSS software. Result significance was assessed using *t*-tests and one-way analysis of variance (ANOVA).

3. Results

3.1. Fruiting body identified the S. vaninii strain

Samples of fruiting bodies (Fig. 1A) were collected randomly from the cultivation greenhouse (Fig. 1B) at Yanbian Xinglin Biotechnology Co., Ltd. Morphological and molecular biological methods were utilized to identify the samples. PCR results (Fig. 1C) and fungal DNA sequencing confirmed that the strain belonged to the family of *Sanghuangporus*

Table 1
List of qPCR primers used in the study.

Target Gene	Primer name	Primer sequence
Bax	Bax F	5′-CAAACTGGTGCTCAAGGCCC-3′
	Bax R	5′-GAGACAGGGACATCAGTCGC-3′
Bcl-2	Bcl-2 F	5`-CGGTTCAGGTACTCAGTCATC-3`
	Bcl-2 R	5`-CGGTGGGGTCATGTGTGTG-3`
P53	P53 F	5′-GTTCCGAGAGCTGAATGAGG-3′
	P53 R	5′-TTATGGCGGGAGGTAGACTG-3′
Caspase-3	Caspase-3 F	5′-CAAACTTTTTCAGAGGGGATCG-3′
	Caspase-3 R	5′-GCATACTGTTTCAGCATGGCA-3′
Caspase-9	Caspase-9 F	5′-CGAACTAACAGGCAAGCAGC-3′
	Caspase-9 R	5′-ACCTCACCAAATCCTCCAGAAC-3′
MMP-2	MMP-2 F	5′-ACCAAGAACTTCCGCCTGTC-3′
	MMP-2 R	5′-TTCGCCAGATGAATCGGTCC-3′
MMP-9	MMP-9 F	5′-CAGACCTTTGAGGGCGAACT-3′
	MMP-9 R	5′-TACCCATCTCCGTGCTCTCT-3′
β-Actin	β-Actin F	5′-AGAGCTACGAGCTGCCTGAC-3′
	β-Actin R	5′-AGCACTGTGTTGGCGTACAG-3′

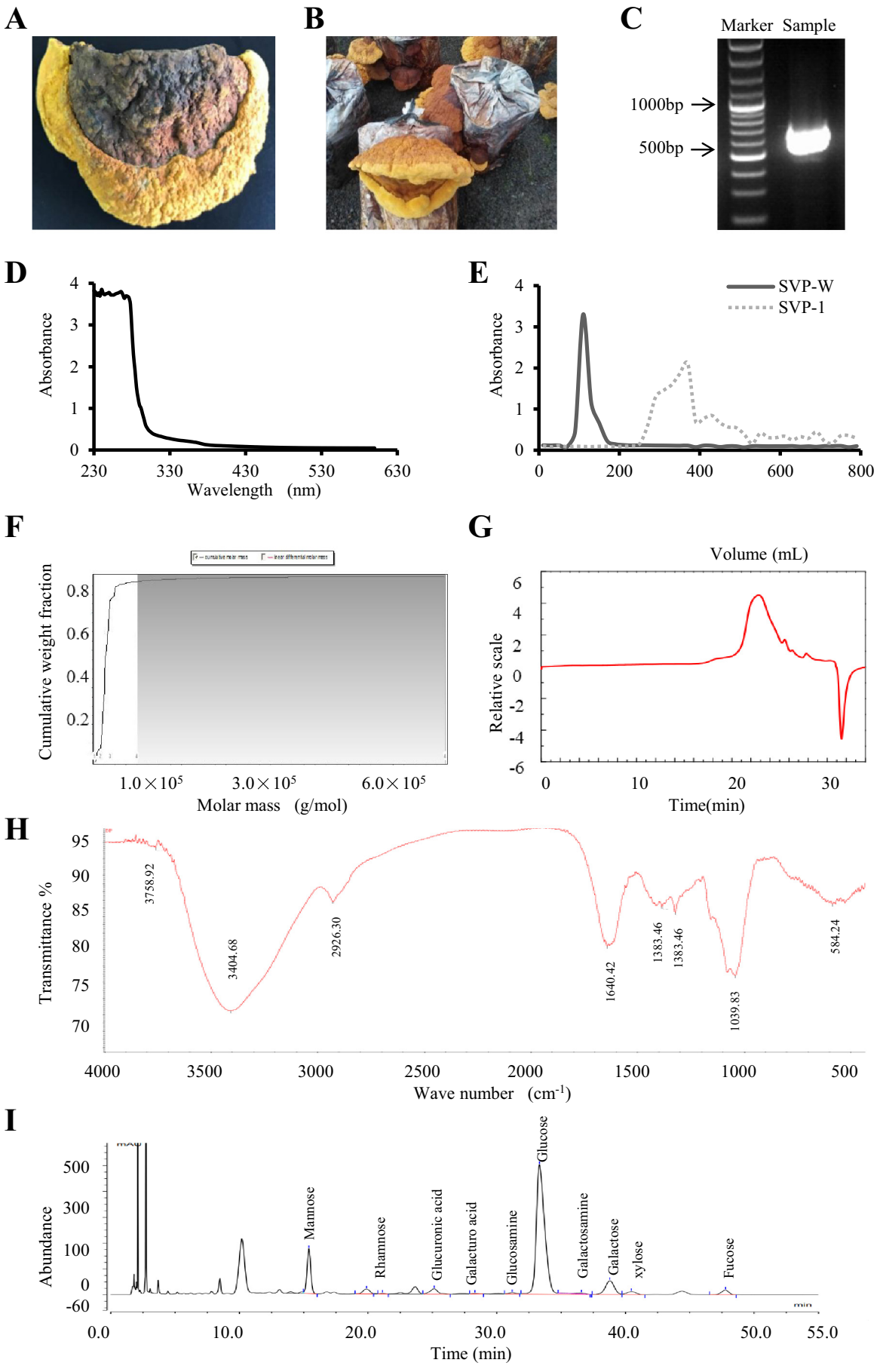
A
B
C
Marker Sample
1000bp
500bp
D
Absorbance
Wavelength (nm)
E
SVP-W
SVP-1
Absorbance
F
Cumulative weight fraction
Molar mass (g/mol)
G
Volume (mL)
Relative scale
Time(min)
H
Transmittance %
3758.92
3404.68
2926.30
1640.42
1383.46
1383.46
1039.83
584.24
Wave number (cm-1)
I
Abundance
Mannose
Rhamnose
Glucuronic acid
Galacturo acid
Glucosamine
Glucose
Galactosamine
Galactose
xylose
Fucose
Time (min)

Table 2
Detection and distribution data for SVP molecular weight.

Molecular weight range g/mol	Content
4100.0– 15,000.0 g/mol	7.7%
15,000.0– 32,000.0 g/mol	79.2%
32,000.0– 80,000.0 g/mol	10.1%
80,000.0– 634,202.0 g/mol	2.9%
Mw	3.156×10^4 g/mol

after sequence alignment using the NCBI website. The ITS sequence was uploaded to the GeneBank (MT299735).

3.2. Characteristic analysis of polysaccharide isolated from S. vaninii

3.2.1. Extraction yield and molecular weight of polysaccharide isolated from S. vaninii

The polysaccharide was extracted from the fruiting body of *S. vaninii* using the boiling water method, and its purity was evaluated by UV spectrometry. The protein content was determined using the Bradford method. The results showed that sample polysaccharide extraction yield was 2.92%. The polysaccharide sample contained less than 0.43% of protein. The purified polysaccharide extract was not contaminated with DNA and RNA (Fig. 1D). In addition, DEAE-cellulose DE-52 and Sephadex G200 purification results indicated that the samples contained neutral (SVP-W) and acid polysaccharides (SVP-1) (Fig. 1E). The molecular weight of SVP was 3.156×10^4 Da using the GPC method (Table 2). The molecular weight distribution of SVP is shown in Fig. 1F–G.

3.2.2. FT-IR spectra for polysaccharide isolated from S. vaninii

After the extraction of the polysaccharide component, FT-IR spectroscopy was used to detect structural characteristics of the extracted samples. The results showed absorbance in different zones with a typical characteristic sugar absorption peak (Fig. 1H). The intense absorption band near 3600–3200 cm^{-1} indicated intermolecular and internal hydrogen bonds. The characteristic spectrum of the main substituents on the sugar chain consists of intermolecular and internal hydrogen bonds, which make the sugar hydroxyl group have a wide peak at 3600–3200 cm^{-1}. Peaks at 3404 cm^{-1} and 2926 cm^{-1} represent hydroxyl (-OH) and C—H, respectively [30–31]. A vibration peak near 1640–1600 cm^{-1} represents the contraction vibration of C═O in the carboxyl group and polysaccharide water and vibration peak. Bands observed at 1730 cm^{-1} and 1640 cm^{-1} indicate that the glucuronic acid component in the extract may be acidic-linked glucan. There was a band near 1400–1430 cm^{-1}, which was the C—H angular vibration absorption of the methyl group connected to the carboxyl group. Carboxymethylated polysaccharides were the bands near 1383 cm^{-1} and 1331 cm^{-1}. Moreover, 1159 cm^{-1} is the ether bond absorption peak of the pyranose ring and the C—O vibration peak of C-O-C [32]. Bands observed at 1100–1010 cm^{-1} represent typical pyranoside stretching vibration [33]. The bands near 1076 cm^{-1} and 1039 cm^{-1} are the angular vibration absorption peaks of pyranose cyclic hydroxyl, indicating that monosaccharides exist in the form of pyranose. All data above are characteristic absorption peaks of sugar.

3.2.3. Monosaccharide composition of polysaccharide isolated from S. vaninii

In order to clarify the composition of the extracted SVP, monosaccharide composition was further tested in each sample. It was mainly composed of mannose, rhamnose, glucuronic acid, galacturonic acid, glucosamine, glucose, galactosamine, galactose, xylose, arabinose, and fucose in molar ratios of 1.63:0.04:0.36:0.03:0.13:8.39:0.08:1.08:0.25:1.07:0.40 (Table 3, Fig. 1I).

3.3. S. vaninii polysaccharide anti-proliferation activity in vitro

To study the antitumor effects of SVP, four cell lines were selected: cervical carcinoma HeLa, glioma SHG-44, hepatocellular carcinoma SMMC-7721, and breast cancer MCF-7 cells. The CCK-8 method was used to detect the inhibitory effect of SVP at different concentrations on the proliferation of these four tumor cell lines. A basic experiment was performed to determine the experimental concentration. According to the results, SVP was considered at different concentrations of 100, 200, 400, 600, and 800 μg/mL. The cytotoxicity effect was expressed using percentage of cell inhibition after 24- and 48-h exposure to different concentrations of SVP.

Results of the SVP CCK-8 assay showed different effects on four cell lines (Fig. 2A–D). SVP showed the strongest inhibitory effect at 600 μg/mL (69.26 ± 1.36%) in MCF-7 breast cancer cells after 48 h. This effect occurred at 800 μg/mL (27.75 ± 0.76%) in cervical carcinoma HeLa cells, 100 μg/mL (50.41 ± 0.41%) in glioma SHG-44 cells, and 600 μg/mL (38.46 ± 2.15%) in hepatocellular carcinoma SMMC-7721 cells. The IC_{50} values were then calculated (Table 4). The inhibitory rate of SVP in MCF-7 cells was the highest and the IC_{50} value (367.64 ± 8.58 μg/mL) was the lowest for 48 h compared to other cells. Comparing the inhibitory ability of SVP in four tumor cell types showed that it was higher in MCF-7 cells than in other cell types (Fig. 2E). The maximum inhibitory ability was reached at a concentration of 400 μg/mL. Therefore, MCF-7 cells were selected for further study and the SVP concentration was set at 400 μg/mL.

Light microscopy results demonstrate that with the increase of SVP concentration and dose time, the number of cells decreased, cell morphology changed, cells shrank into clusters, cell fragmentation occurred, and cell fragments floated in the medium (Fig. 3A). SVP inhibition of cell proliferation was observed using crystal violet staining. With the increase of SVP concentration, cell proliferation was significantly inhibited and cell density was significantly decreased compared to the control group.

To further determine the influence of SVP on MCF-7 cell growth, colony formation assay was carried out. The colony formation ability of tumor cells is also a prerequisite for the evaluation of tumor cell migration, which can be used to evaluate whether drugs can inhibit tumor cells from forming new lesions in a human body. SVP inhibited colony formation in a concentration-dependent manner compared to the control group ($p < 0.01$ and $p < 0.001$; Fig. 3B–C).

3.4. S. vaninii polysaccharide mediated G2/M phase cell cycle arrest in MCF-7 cells

Cell cycle regulation is one of the factors affecting cell proliferation. Therefore, cell cycle after SVP treatment was evaluated and cell cycle changes were analyzed using flow cytometry. Results are shown in Fig. 3D. Compared to the untreated group, cells in the G0/G1 phase decreased from 47.11% to 36.32% and accumulated in the G2/M phase from 16.24% to 24.96% at SVP concentration of 400 μg/mL. A decrease in the S phase was also present, with cell percentages changing from 29.45 ± 4.38% to 10.63 ± 3.97% (Fig. 3E). These results suggest that SVP mainly arrested MCF-7 cells in the G2/M phase. After 24 h of SVP treatment, the results indicated that SVP mediated the G2/M phase

Fig. 1. *S. vaninii* sample identification information and SVP component characteristics identification. (A) Sample photo; (B) Sample culture environment; (C) Agarose gel electrophoresis for identification of fungal species; (D) SVP ultraviolet absorption spectrum; (E) Neutral (SVP-W) and acid polysaccharides (SVP-1) in SVP were separated by DEAE cellulose DE-52 ion exchange column and the content of polysaccharide was determined by phenol-sulfuric acid method; (F–G) SVP molecular weight distribution; (H) SVP FT-IR spectra; (I) Monosaccharide composition of SVP.

Table 3
Monosaccharide component in SVP molar ratio.

Monosaccharide	mannose	rhamnose	glucuronic acid	galacturonic acid	glucosamine	glucose	galactosamine	galactose	xylose	arabinose	fucose
Molar ratio	1.63	0.04	0.36	0.03	0.13	8.39	0.08	1.08	0.25	1.07	0.40

cell cycle arrest in MCF-7 cells ($p < 0.05$ and $p < 0.01$). Additionally, the proportion of apoptotic cells increased from 4.12% to 25.56%, indicating that SVP promotes MCF-7 cell apoptosis (late apoptosis and dead cells). Then, flow cytometry was used to assess the proportion of apoptotic cells at different stages.

3.5. S. vaninii polysaccharide induced MCF-7 cell apoptosis

The unlimited proliferation of tumor cells is another important factor in tumor development. If SVP can promote tumor cell apoptosis and has the ability to initiate programmed apoptosis of tumor cells, it

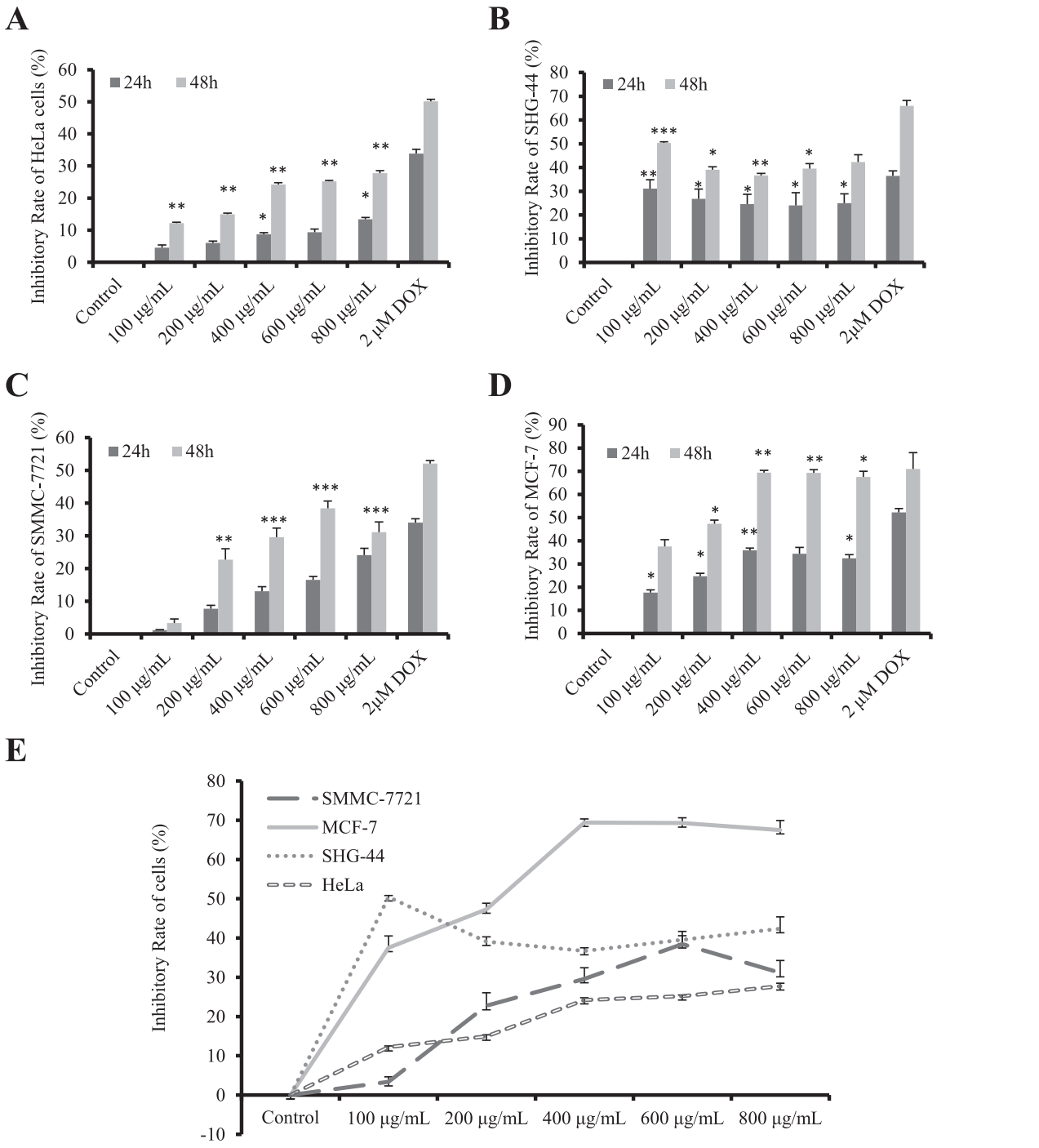

Fig. 2. Effect of SVP on four different tumor cell lines. (A–D) Antitumor effects on HeLa, SHG-44, SMMC-7721, and MCF-7 cell lines; (E) Comparison of SVP tumor inhibition ability in four cell lines at 48 h.

Table 4
IC_{50} concentration of SVP in tumor cell lines.

		HeLa	SHG-44	SMMC-7721	MCF-7
IC_{50} (μg/mL)	24 h	2110.62 ± 128.02	4182.97 ± 1619.85	1122.23 ± 56.46	983.32 ± 107.47
	48 h	1130.46 ± 16.69	1017.57 ± 110.38	896.96 ± 39.04	367.64 ± 8.58

Data are presented as mean ± SEM ($n \geq 3$).

is important to study it in the future. Combined with flow cytometry and detection results (Fig. 3F–G), cells were mostly alive in the control group with very few dead cells present (1.2%). After treatment with SVP, the rate of cells entering the apoptotic phase was significantly higher going from 6.1% up to 51.8% ($p < 0.01$ and $p < 0.001$). The proportion of living cells decreased from 92.7% to 47.5%. These results suggested obvious pro-apoptotic effects of SVP in MCF-7 cells at 24 h. At SVP concentration of 400 μg/mL and treatment for 24 h (three parallel tests), the percentage of Q2, Q4, and their sum increased from 6.77 ± 0.34% to 37.24 ± 2.72% ($p < 0.01$). This suggested that SVP mediated the apoptosis of MCF-7 cells after 24 h of treatment.

3.6. S. vaninii polysaccharide limits MCF-7 cell migration and invasion

Metastasis and invasion are the difficulties of tumor treatment. Therefore, a series of studies on the effect of SVP in MCF-7 cells was carried out. Scratch wound healing assay was utilized to evaluate the ability of SVP to inhibit tumor cell migration. Results showed that MCF-7 cells covered the scratch area after 24 and 48 h, while SVP treatment group scratch area was unhealed (Fig. 4A–B). Transwell chamber experiment schematic is shown in Fig. 4C. Tumor cells were directly inoculated in the chamber. They then gradually migrated to the medium with serum, while the lower chamber with SVP significantly inhibited the migration ability of cells. Fewer cells migrated across the membrane (Fig. 4D–E). Matrigel was also placed in the small chamber and the cells were cultured under the same conditions to explore the anti-invasion effect of SVP. The results showed that SVP can significantly inhibit breast cancer MCF-7 cells through the membrane and the Matrigel in the lower chamber compared to the cells in the control group (Fig. 4F–G).

3.7. S. vaninii polysaccharide affects gene expression in apoptotic signaling pathway

The above results showed that SVP can induce apoptosis in MCF-7 cells and that cell cycle arrest and inhibition of migration and invasion are results of precise regulation by a series of genes. Thus, mRNA expression was further examined in MCF-7 cells (Fig. 5A). The results of qPCR showed that p53 mRNA was significantly increased in SVP-treated MCF-7 cells. Transcripts of p53 target genes, such as Bax and p21, were augmented by the qPCR analysis in MCF-7 cells. Bax and p53 mRNA increased, while Bcl-2 decreased following SVP treatment ($p < 0.05$ and $p < 0.001$). This further indicated that SVP induces apoptosis in MCF-7 cells, probably via the Bcl-2/Bax pathway. Subsequently, caspase-3 and caspase-9 were assessed according to the p53-mediated signaling pathway and the results all showed that SVP plays a role in promoting tumor cell apoptosis. Then, we speculate the signaling pathway for SVP in MCF-7 cells. (See Fig. 6)

In order to further clarify the mechanism of the antitumor effect, the expression levels of tumor-related proteins were detected by Western blotting. Apoptosis-related protein caspase-3, cleaved caspase-3, caspase-9, cleaved caspase-9, caspase-8, Bax, and p53 expression was significantly increased and that of Bcl-2 and PARP was reduced (Fig. 5B–E).

In addition, p21 may play a pro-apoptotic role in either p53-dependent or -independent manner. It has been suggested that p21 is a negative regulator of p53-dependent apoptosis [34]. Thus, an important member of the cyclin-dependent kinase inhibitor family p21 was examined. After SVP treatment, p21 expression increased. Both p21 and p53 can jointly form the G1 checkpoint in the cell cycle, which cannot be passed without repair after DNA damage, reducing the replication and accumulation of damaged DNA and thus playing an anticancerous role (Fig. 6).

3.8. S. vaninii polysaccharide decreased MMP-2 and MMP-9 expression in MCF-7 cells

Cancer cell migration and invasion factor research has attracted much attention in recent years. MMP-2 and MMP-9 belong to the MMP family and are related to the degradation of extracellular membrane components. According to the previous results, SVP also significantly inhibited the migration of tumor cells. Therefore, MMP-2 and MMP-9 mRNA was detected in the MCF-7 cells. The results showed that MMP-2 and MMP-9 mRNA was decreased significantly after the SVP treatment (Fig. 5A). This also suggests that SVP may inhibit secretion of the MMP family members in MCF-7 cells, thus limiting tumor cell migration and invasion to other organs in the body ($p < 0.001$).

MMP-2 and MMP-9 protein expression in the MMP family was detected by Western blotting. Both of them are major components of hydrolyzed degenerated collagen and type IV collagen of the basal membrane and participate in changing intercellular adhesion, destroying the histological barrier of tumor cell invasion, and inhibiting tumor invasion and metastasis. MMP-2 and MMP-9 protein expression was decreased significantly compared to the control group (Fig. 5B–C). This indicates that SVP influences the transmembrane metastatic ability of MCF-7 cells to inhibit tumor invasion (Fig. 6).

4. Discussion

SVP with a molecular weight of 3.156×10^4 Da and composed of neutral and acidic polysaccharides was extracted and purified from the fruiting body of traditional Chinese medicine *S. vaninii*. *Sanghuangporus* has been used as a traditional medicine for cancer therapy in some Asian countries. Artificial cultivation of *S. vaninii* has been realized after many years of cultivation efforts. However, the antitumor *S. vaninii* mechanism is still not completely understood.

The purpose of this research was to explain the effects and underlying mechanism of *S. vaninii* polysaccharides in tumor cells in vitro. As a result, SVP showed various degrees of antitumor activity in four cell lines, including HeLa, SHG-44, SMMC-7721, and MCF-7 cells. This activity was especially prominent in MCF-7 cells, which is indicative of SVP as a potential antitumor ingredient. The effect of SVP on MCF-7 cells is time-dependent and dose-dependent. SVP had a significant effect on apoptosis, metastasis, and invasion of tumor cells. Genes, such as p53, Bax, Bcl-2, MMP-2, MMP-9, and caspase-3, −8, and − 9 were significantly up-regulated or down-regulated after SVP treatment.

In many cancers, high rates of metastasis and recurrence are difficult to treat. Radiotherapy and chemotherapy are commonly used to treat tumors [35]. However, these methods are expensive and the damage to the body is very serious and sometimes irreversible. Therefore, drugs that are more effective need to be investigated. Natural products have been used for the treatment of many bodily ailments for centuries. However, the associated mechanisms remain poorly understood [36]. Macrofungi have become a hot topic in recent years. Fungal polysaccharides have been found to have potential medicinal ingredients, such as *G. lucidum* [37], *P. linteus* [38–39], and *L. edodes* [40] polysaccharides.

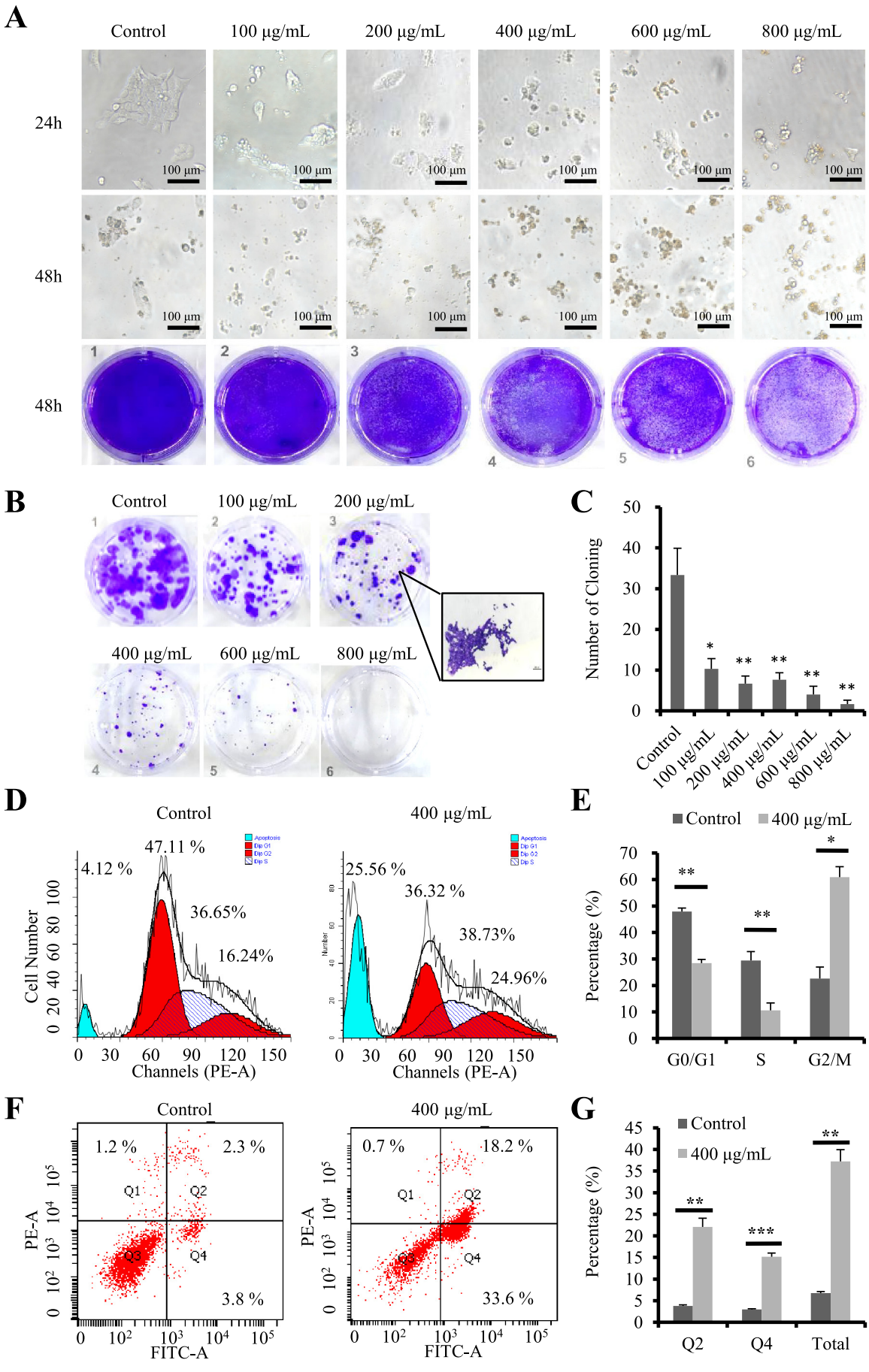
A
Control
100 μg/mL
200 μg/mL
400 μg/mL
600 μg/mL
800 μg/mL
24h
48h
48h
100 μm
B
Control
100 μg/mL
200 μg/mL
400 μg/mL
600 μg/mL
800 μg/mL
C
Number of Cloning
Control
100 μg/mL
200 μg/mL
400 μg/mL
600 μg/mL
800 μg/mL
D
Control
400 μg/mL
47.11 %
4.12 %
36.65%
16.24%
25.56 %
36.32 %
38.73%
24.96%
Cell Number
Channels (PE-A)
E
Control
400 μg/mL
Percentage (%)
G0/G1
S
G2/M
F
Control
400 μg/mL
1.2 %
2.3 %
3.8 %
0.7 %
18.2 %
33.6 %
Q1
Q2
Q3
Q4
PE-A
FITC-A
G
Control
400 μg/mL
Percentage (%)
Q2
Q4
Total

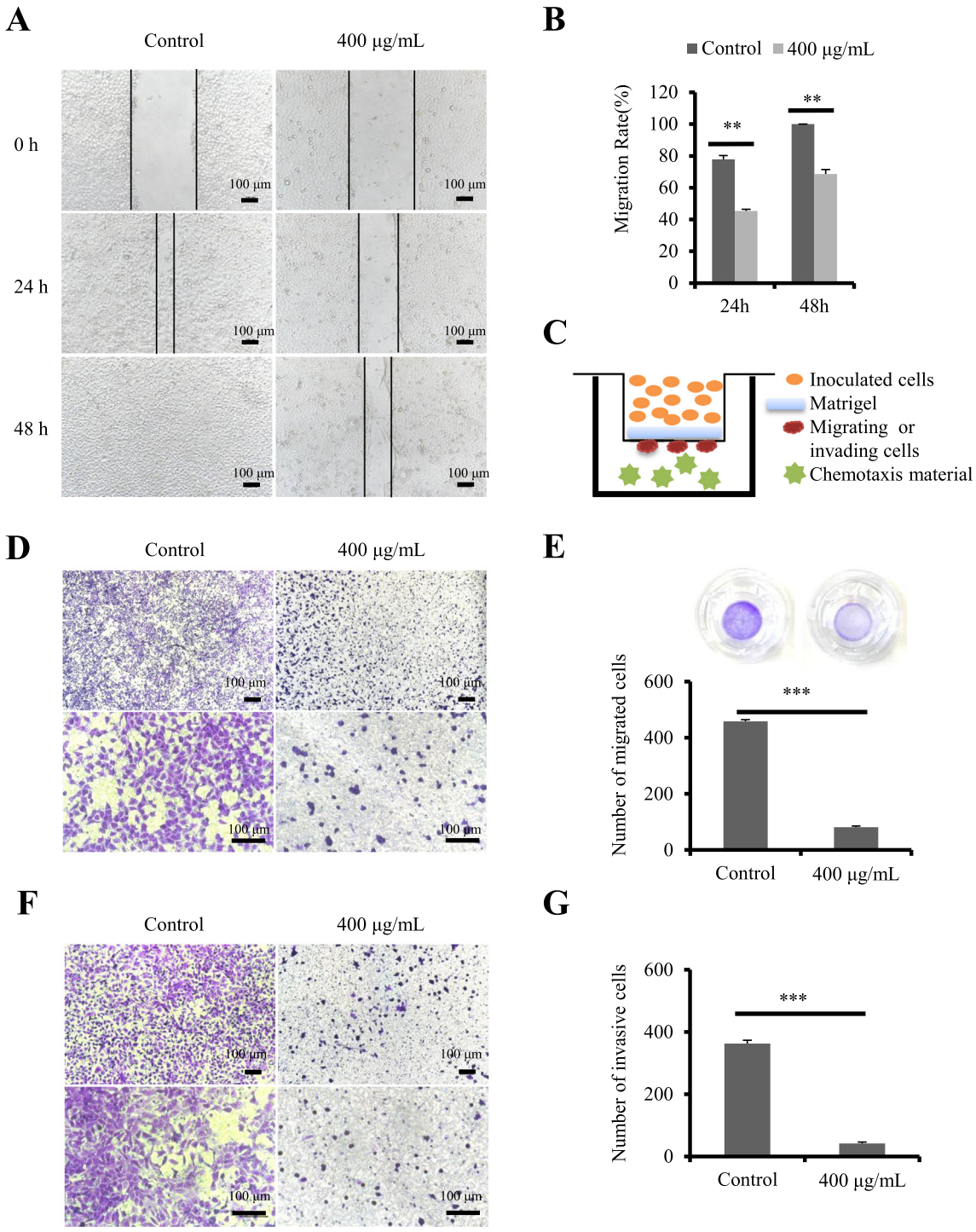

Fig. 4. Changes in MCF-7 cell migration and invasion after 0- and 400-μg/mL SVP treatment. (A–B) MCF-7 cell scratch wound healing assay after SVP treatment; (C) Transwell chamber experimental diagram; (D–G) MCF-7 cell migration and invasion after SVP treatment. Mean ± SEM, n ≥ 3; $^{*}p < 0.05$; $^{**}p < 0.01$; $^{***}p < 0.001$ compared to the control group.

In the study of antitumor drug effects, cell cycle regulation is an important factor in the development of tumors. *Grifola frondosa* is a widely consumed and medicinal fungus. Polysaccharide extracted from *G. frondosa* inhibited HepG2 cell proliferation and S phase arrest [41]. The above results indicate that medicinal fungi have excellent antitumor activity. Inhibiting tumor cell proliferation and inducing apoptosis might be a common fungal polysaccharide mechanism responsible for its anti-tumor effect [42]. The p53 tumor suppressor is a transcription factor that regulates cell growth and death in response to environmental stimuli, such as DNA damage [43]. Many studies

Fig. 3. Antitumor effects at different concentrations of SVP in MCF-7 cells. (A) Cell Morphologic of 24–48 h and cell density changes in MCF-7 cells treated with different concentrations of SVP; (B—C) Detection of colony formation unit ability in MCF-7 cells after treatment with different concentrations of SVP for 21 days; (D–E) Cell cycle changes after SVP treatment detected by flow cytometry; (F–G) Flow cytometry was used to detect MCF-7 cell apoptosis after SVP treatment; Mean ± SEM, $n \geq 3$; $^{*}p < 0.05$; $^{**}p < 0.01$; $^{***}p < 0.001$ compared to the control group.

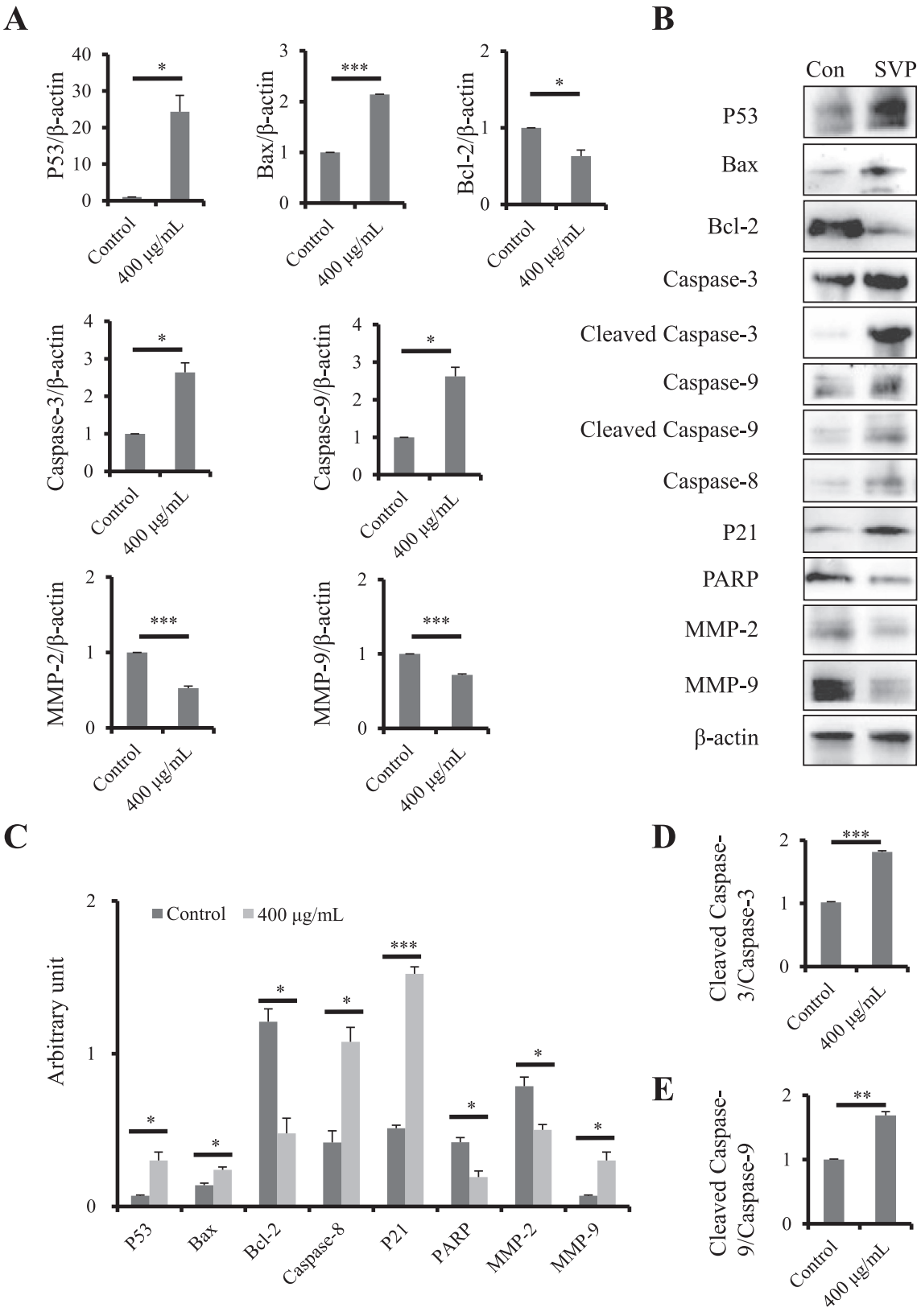

Fig. 5. Proposed mechanism for the effects of SVP on MCF-7 cells. (A) Bax, Bcl-2, p53, caspase-3, caspase-9, MMP-2, and MMP-9 mRNA expression analysis; (B—C) Detection of SVP in tumor-related protein expression in MCF-7 cells by Western blotting; (D) Change in the ratio of expressions of cleaved caspase-3 and caspase-3 after treatment with SVP; (E) Change in the ratio of expressions of cleaved caspase-9 and caspase-9 after treatment with SVP. Mean ± SEM, n ≥ 3; $^{*}p < 0.05$; $^{**}p < 0.01$; $^{***}p < 0.001$ compared to the control group.

have reported that p53 plays a vital role in inducing cell cycle arrest, as well as blocking the G2/M phase and reducing the expression of cyclin D4, while increasing the expression of CDK inhibitor p21 compared to a control group [44]. Ginger polysaccharides induce apoptosis and up-regulate the expression of p53 in human hepatocellular carcinoma HepG2 cells [45]. *Hericium erinaceus* polysaccharide protein HEG-5 up-

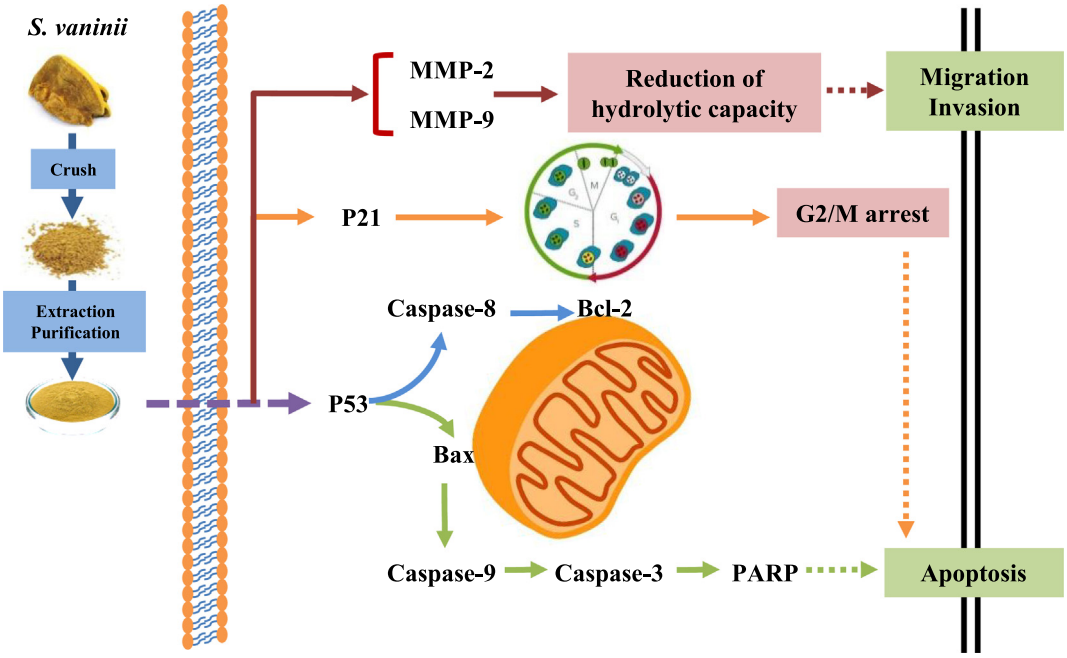

Fig. 6. A series of antitumor mechanism pathways for SVP in MCF-7 cells.

regulated the expression of p53 in human SGC-7901 cells to realize the regulation of apoptosis [46]. Tumor suppressor p53 is associated with the expression of many regulation-related genes, with mutations occurring in more than 50% of malignancies. Many p53 target genes are involved in apoptosis [47]. In recent years, the p53 signaling pathway has been gradually identified. In the present study, many tumor-related gene mRNAs and proteins were detected. Levels of p53, Bax, caspase-3, -8, and -9, and p21 were increased by SVP, demonstrating that SVP activates apoptosis and cell cycle arrest in MCF-7 cells. Also, Bcl-2 and PARP expression levels were decreased significantly. Therefore, it is possible that SVP can interact with tumor cells to target p53 to suppress MCF-7 cell proliferation and induce cell apoptosis. Thus, it was probably associated with the p53-related signaling pathway.

Matrix metalloproteinases (MMPs) have become the focus of research due to their ability to inhibit tumor cell invasion and metastasis [48]. Moreover, SVP was also found to play a very significant inhibitory role in the migration and invasion of tumor cells via MMP-2 and MMP-9. The results indicated that SVP can effectively inhibit MCF-7 cell migration and invasion in vitro. This action probably occurs via degradation of the extracellular matrix to inhibit MCF-7 cell migration and invasion. The MMPs constitute a multigene family of over 25 secreted and cell surface enzymes that process or degrade numerous extracellular matrices. Their targets include other proteinases, proteinase inhibitors, clotting factors, chemotactic molecules, latent growth factors, growth factor-binding proteins, cell surface receptors, cell-cell adhesion molecules, and virtually all structural extracellular matrix proteins [49]. Many of their domains play an essential role in the localization of several important proteolytic events to specific regions of the cell surface. Many fungal polysaccharides, like *Trametes versicolor* and *G. frondosa* polysaccharides, also regulate the migration and invasion of tumor cells by inhibiting the expression of MMPs. A decrease in MMP-2 enzyme activity, a crucial MMP important for the degradation of the extracellular matrix in polysaccharides, has also been detected in human colon cancer, LoVo, and HT-29 cells [50]. Chinese medicine CGA formula consists of a polysaccharide from *Cordyceps sinensis* mycelia, gypenosides, and amygdalin, which are derived from the Fuzheng Huayu capsule for treating liver fibrosis. After treatment, MMP-2 and MMP-9 protein levels were decreased [51]. Therefore, SVP is probably involved in tumor cell migration and invasion by inhibiting MMPs.

Nevertheless, the complexity of polysaccharide components can lead to differences in structure and composition due to differences in extraction methods, storage conditions, and separation and purification methods. These reasons lead to the diversity of polysaccharide components from the same plant or fungus. In addition, detailed analysis of polysaccharide composition and structure is limited, which indirectly leads to the lack of in-depth understanding of the biological activities of polysaccharides. Therefore, standard polysaccharide extraction methods and in-depth analyses of the structure and mechanism need to be investigated in the future.

Polysaccharides are the major active component in mushrooms and fungi, which can enhance innate and cell-mediated immune responses and exhibited good antitumor activity in animals and humans [52]. According to the literature, many kinds of polysaccharides have been tested in animals, such as *Glycyrrhiza uralensis* polysaccharide [53], *Panax ginseng* polysaccharide [54], *Helicteres angustifolia* polysaccharide [55], *Coriolus versicolor* polysaccharide [56,57], Lentinan from *Lentinula edodes* [58], and *Ganoderma lucidum* polysaccharide [59]. Therefore, we believe that *Sanghuangporus vaninii* polysaccharide also has experimental prospects in mammary tumor animal models in vivo.

According to these research results, it is believed that SVP is one of the active components of the anti-tumor *S. vaninii* effect, although a more detailed study of the gene regulation mechanism is needed.

5. Conclusion

In this study, SVP was extracted and its characteristics were described. SVP antitumor activities were evaluated in four human cancer cell lines. The extracted SVP demonstrated excellent tumor inhibition in MCF-7 cell lines. It significantly inhibited the proliferation of MCF-7 cells and G2 phase cell arrest, promoted tumor cell apoptosis, and significantly inhibited tumor cell migration and invasion in vitro. SVP plays an antitumor role via the p53 signaling pathway and inhibits the production of MMPs. We expect that our results will serve as evidence to support the use of SVP as an antitumor adjuvant in breast cancer patients.

Author statement

Yu Li: Conceptualization, Supervision. Qi Wang: Resources, Funding acquisition. Andrey A. Gontcharov: Methodology. Xilin Wan: Investigation, Writing - Original draft preparation and Editing, Xin Jin: Visualization, Writing - Reviewing. Mengle Xie: Software. Jie Liu: Methodology. Huan Wang: Software. Ruina Lv: Validation. Daiyao Liu: Software.

Funding

This work was supported by the China Agriculture Research System (CARS-20-08B), the Program of Science and Technology Development Program of Jilin Province (20180414079GH), the Program of Jilin Forestry and Grassland Department (JLT2017-01), the Shandong Taishan Leading Talents Project (LJNY201611), and the 111 Project (D17014).

Acknowledgement

We thank Profs. Shuying Liu and Changbao Chen from Jilin Ginseng Academy of Changchun University of Chinese Medicine for building the cytology experiment platform and providing equipment and space for follow-up experiments. We also thank the research group of Profs. Xiaojuan Zhu and Min Wei from the School of Life Sciences, Northeast Normal University for providing laboratory space and equipment.

Declaration of competing interest

The authors declare no conflict of interest.

References

[1] R.L. Siegel, K.D. Miller, A. Jemal, Cancer statistics, 2019, CA Cancer J. Clin. 69 (1) (2019) 7–34https://doi.org/10.3322/caac.21551.
[2] G.P. Gong, Q. Liu, Y.N. Deng, et al., Arabinogalactan derived from *Lycium barbarum* fruit inhibits cancer cell growth via cell cycle arrest and apoptosis, Int. J. Biol. Macromol. 149 (2020) 639–650https://doi.org/10.1016/j.ijbiomac.2020.01.251.
[3] N. Wang, J.Y. Yang, J.G. Lu, et al., A polysaccharide from Salvia miltiorrhiza Bunge improves immune function in gastric cancer rats, Carbohydrate Polymers. 111 (2014) 47–55https://doi.org/10.1016/j.carbpol.2014.04.061.
[4] Y.R. Dong, S.J. Cheng, J.H. Qi, et al., Antimicrobial and antioxidant activities of *Flammulina velutipes* polysacchrides and polysacchride-iron(III) complex, Carbohyd. Polym. 161 (2017) 26–32https://doi.org/10.1016/j.carbpol.2016.12.069.
[5] S.T. Fan, S.P. Nie, X.J. Huang, et al., Protective properties of combined fungal polysaccharides from *Cordyceps sinensis* and *Ganoderma atrum* on colon immune dysfunction, Int. J. Biol. Macromol. 114 (2018) 1049–1055https://doi.org/10.1016/j.ijbiomac.2018.04.004.
[6] W.Y. Li, J.L. Wang, H.P. Hu, et al., Functional polysaccharide lentinan suppresses human breast cancer growth via inducing autophagy and Caspase-7-mediated apoptosis, J. Funct. Foods. 45 (2018) 75–85https://doi.org/10.1016/j.jff.2018.03.024.
[7] Y.L. Tian, Y.H. Yi, L. Bai, et al., Lentinan in-situ coated tungsten oxide nanorods as a nanotherapeutic agent for low power density photothermal cancer therapy, Int. J. Biol. Macromol. 137 (2019) 904–911https://doi.org/10.1016/j.ijbiomac.2019.06.183.
[8] G.M. Ren, L.M. Xu, T.Y. Lu, et al., Structural characterization and antiviral activity of lentinan from *Lentinus edodes* mycelia against infectious hematopoietic necrosis virus, Int. J. Biol. Macromol. 115 (2018) 1202–1210https://doi.org/10.1016/j.ijbiomac.2018.04.132.
[9] H.K. Bao, L.J. Sun, Y. Zhu, et al., Lentinan produces a robust antidepressant-like effect via enhancing the prefrontal Dectin-1/AMPA receptor signaling pathway, Behav. Brain. Res. 317 (2017) 263–271https://doi.org/10.1016/j.bbr.2016.09.062.
[10] L.N. Cui, J.Y. Wang, R. Huang, et al., Cordyceps sinensis Polysaccharide Inhibits Colon Cancer Cells Growth by Inducing Apoptosis and Autophagy Flux Blockage via mTOR Signaling, 128, 2019 459–467https://doi.org/10.1016/j.ijbiomac.2019.01.129.
[11] W. Jia, J. Feng, J.S. Zhang, et al., Structural characteristics of the novel polysaccharide FVPA1 from winter culinary-medicinal mushroom, *Flammulina velutipes* (Agaricomycetes), capable of enhancing natural killer cell activity against K562 tumor cells, Int. J. Med. Mushrooms. 19 (2017) 535–546https://doi.org/10.1615/IntJMedMushrooms.v19.i6.50.
[12] W.H. Chen, H.Y. Tan, Q. Liu, et al., A Review: The Bioactivities and Pharmacological Applications of *Phellinus linteus*, Molecules. 24 (2019) 1888https://www.mdpi.com/1420-3049/24/10/1888.
[13] L. Chen, J.Z. Pan, X. Li, et al., Endo-polysaccharide of *Phellinus igniarius* exhibited anti-tumor effect through enhancement of cell mediated immunity, Int Immunopharmacol. 11 (2) (2011) 255–259.
[14] M.E. Balandaykin, I.V. Zmitrovich, Review on Chaga medicinal mushroom, *Inonotus obliquus* (higher Basidiomycetes): realm of medicinal applications and approaches on estimating its resource potential, Int. J. Med. Mushrooms. 17 (2015) 95–104https://doi.org/10.1615/intjmedmushrooms.v17.i2.10.
[15] K.W. Oh, C.K. Lee, Y.S. Kim, et al., Antiherpetic activities of acidic protein bound polysacchride isolated from *Ganoderma lucidum* alone and in combinations with acyclovir and vidarabine, J. Ethnopharmacol. 72 (2000) 221–227https://doi.org/10.1016/S0378-8741(00)00254-3.
[16] L. Zhu, J. Song, J.L. Zhou, et al., Species diversity, phylogeny, divergence time, and biogeography of the genus *Sanghuangporus* (Basidiomycota), Front. Microbiol. 10 (2019) 812https://doi.org/10.3389/fmicb.2019.00812.
[17] S.H. Wu, Y.C. Dai, T. Hattori, et al., Species clarification for the medicinally valuable 'sanghuang' mushroom, Botanical Studies. 53 (2012) 135–149http://ejournal.sinica.edu.tw/bbas/content/2012/1/Bot531-13.pdf.
[18] Index fungorum, Intraspecific search of *sanghuangporus*, http://www.indexfungorum.org/Names/Names.asp 2020 (accessed 3 April 2020).
[19] Z. Zhang, G. Lv, J. Cheng, et al., Characterization and biological activities of polysaccharides from artificially cultivated *Phellinus baumii*, Int. J. Biol. Macromol. 129 (2019) 861–868, https://doi.org/10.1016/j.ijbiomac 2019.02.082.
[20] S. Lee, D. Lee, T.S. Jang, et al., Anti-inflammatory phenolic metabolites from the edible fungus *Phellinus baumii* in LPS-stimulated RAW264.7 Cells, Molecules 22 (2017) , pii: E1583 http://dx.org/10.3390/molecules22101583.
[21] F.C. Jiang, H.N. Zhang, D. Wu, et al., Kinetic models for the effect of temperature on flavonoid production in liquid submerged fermentation by *Phellinus baumii*, Biotechnol. Appl. Biochem. 65 (2018) 739–747http://dx.org/10.1002/bab.1658.
[22] L. Ye, H. Zheng, Z. Zhang, et al., Preparative isolation of 5 antioxidant constituents from the medicinal mushroom *Phellinus baumii* (Agaricomycetes) by high-speed countercurrent chromatography and preparative high-performance liquid chromatography, Int. J. Med. Mushrooms. 19 (2017) 319–326http://dx.org/10.1615/IntJMedMushrooms.v19.i4.20.
[23] K. Ota, I. Yamazaki, T. Saigoku, et al., Phellilane L, sesquiterpene metabolite of *Phellinus linteus*: Isolation, structure elucidation, and asymmetric total synthesis, J. Org. Chem. 82 (2017) 12377–12385https://doi.org/10.1021/acs.joc.7b02141.
[24] W.H. Yeo, E.I. Hwang, S. So, et al., Phellinone, a new furanone derivative from the *Phellinus linteus* KT&G PL-2, Arch. Pharm. Res. 30 (2007) 924–926http://dx.org/10.1007/bf02993957.
[25] S.C. Huang, P.W. Wang, P.C. Kuo, et al., Hepatoprotective principles and other chemical constituents from the mycelium of *Phellinus linteus*, Molecules. 23 (2018) 1705https://doi.org/10.3390/molecules23071705.
[26] C.J. Lin, H.M. Lien, H.Y. Chang, et al., Biological evaluation of *Phellinus linteus*-fermented broths as anti-inflammatory agents, J. Biosci. Bioeng. 118 (2014) 88–93https://doi.org/10.1016/j.jbiosc.2014.01.001.
[27] Y.S. Lee, Y.H. Kang, J.Y. Jung, et al., Inhibitory constituents of aldose reductase in the fruiting body of *Phellinus linteus*, Biol. Pharm. Bull. 31 (2008) 765–768https://doi.org/10.1248/bpb.31.765.
[28] T.Y. Song, N.C. Yang, C.L. Chen, et al., Protective effects and possible mechanisms of ergothioneine and hispidin against methylglyoxal-induced injuries in rat pheochromocytoma cells, Oxid. Med. Cell. Longev. 2017 (2017) 1–10https://doi.org/10.1155/2017/4824371.
[29] S.C. Huang, P.C. Kuo, H.Y. Hung, et al., Ionone derivatives from the mycelium of *Phellinus linteus* and the inhibitory effect on activated rat hpatic stellate cells, Int. J. Mol. Sci. 17 (2016) 681https://doi.org/10.3390/ijms17050681.
[30] J.M. Yan, L. Zhu, Y.H. Qu, et al., Analyses of active antioxidant polysaccharides from four edible mushrooms, Int. J. Biol. Macromol. 123 (2019) 945–956https://doi.org/10.1016/j.ijbiomac.2018.11.079.
[31] S. Li, N.P. Shah, Antioxidant and antibacterial activities of sulphated polysaccharides from Pleurotus eryngii and Streptococcus thermophilus ASCC 1275, Food Chem. 165 (2014) 262–270http://refhub.elsevier.com/S0141-8130(18)33596-7/rf0150.
[32] R.G. Zhbankov, V.V. Sivchik, T.E. Kolosova, Vibrational spectra of monosaccharides which differ in the configuration of the co(ch) groups, J. Appl. Spectrosc. 32 (1980) 472–477http://refhub.elsevier.com/S0141-8130(18)33596-7/rf0155.
[33] J.Z. He, Q.M. Ru, D.D. Dong, et al., Chemical characteristics and antioxidant properties of crude water soluble polysaccharides from four common edible mushrooms, Molecules 17 (2012) 4373–4387http://refhub.elsevier.com/S0141-8130(18)33596-7/rf0160.
[34] H.Z. Huang, A.Y. Chen, X.Q. Ye, et al., Galangin, a flavonoid from lesser galangal, induced apoptosis via P53-dependent pathway in ovarian cancer cells, Molecules 57 (2020) 1579https://doi.org/10.3390/molecules25071579.
[35] C.H. Chapman, U. Parvathaneni, S.S. Yom, Revisiting induction chemotherapy before radiotherapy for head and neck cancer, part II: nasopharyngeal carcinoma, Future Oncol. 13 (2017) 581–584https://doi.org/10.2217/fon-2016-0544.
[36] X.L. Wan, X. Jin, Y.H. Ren, et al., Antitumor effects and mechanism of protein from *Panax ginseng* C. A. Meyer on human breast cancer cell line MCF-7, Pharmacogn. Mag. 15 (2019) 715–721https://doi.org/10.4103/pm.pm_151_19.
[37] P.J. Zeng, Y.L. Chen, L.J. Zhang, et al., Chapter ten - *Ganoderma lucidum* polysaccharide used for treating physical frailty in China, Prog. Mol. Biol. Transl. Sci. 163 (2019) 179–219https://doi.org/10.1016/bs.pmbts.2019.02.009.
[38] Y.Y. Chai, G.B. Wang, L.L. Fan, et al., A proteomic analysis of mushroom polysaccharide-treated HepG2 cells, Sci. Rep. 6 (2016) 23565–23576https://doi.org/10.1038/srep23565.
[39] T.Q. Yu, S. Ganapathy, L. Shen, et al., A lethal synergy induced by *Phellinus linteus* and camptothecin11 in colon cancer cells, Oncotarget. 9 (2018) 6308–6319http://dx.doi.org/10.18632/oncotarget.23918.
[40] X. Cao, D. Liu, Y. Xia, et al., A novel polysaccharide from *Lentinus edodes* mycelia protects MIN6 cells against high glucose-induced damage via the MAPKs and Nrf2 pathways, Food Nutr Res. 6 (2019) 630https://doi.org/10.29219/fnr.v63.1598.
[41] C. Pei, H.P. Liu, H.H. Ji, et al., A cold-water soluble polysaccharide isolated from *Grifola frondosa* induces the apoptosis of HepG2 cells through mitochondrial

passway, Int. J. Biol. Macromol. 125 (2019) 1232–1241https://doi.org/10.1016/j.ijbiomac.2018.09.098.
[42] H.Y. Xu, L.Y. Liu, M. Ding, et al., Effect of *Ganoderma applanatum* polysaccharides on MAPK/ERK pathway affecting autophagy in breast cancer MCF-7 cells, Int. J. Biol. Macromol. 146 (2020) 353–362https://doi.org/10.1016/j.ijbiomac.2020.01.010.
[43] Y. Sasaki, S. Ishid, I. Morimoto, et al., The P53 family member genes are involved in the Notch signal pathway, 277 (2002) 719–724https://www.jbc.org/content/277/1/719.
[44] A. Arcella, M.A. Oliva, M. Sanchez, et al., Effects of hispolon on glioblastoma cell growth, Environ. Toxicol. 32 (2017) 2113–2123https://doi.org/10.1002/tox.22419.
[45] Y. Wang, S.X. Wang, R.Z. Song, et al., Ginger polysaccharides induced cell cycle arrest and apoptosis in human hepatocellular carcinoma HepG2 cells, Int. J. Biol. Macromol. 123 (2019) 81–90https://doi.org/10.1016/j.ijbiomac.2018.10.169.
[46] X.Y. Zan, F.J. Cui, Y.H. Li, et al., *Hericium erinaceus* polysaccharide-protein HEG-5 inhibits SGC-7901 cell growth via cell cycle arrest and apoptosis, Int. J. Biol. Macromol. 76 (2015) 242–253https://doi.org/10.1016/j.ijbiomac.2015.01.060.
[47] S.B. Lee, S.S. Lee, J.Y. Park, et al., Induction of P53-dependent apoptosis by prostaglandin A_2, Biomolecules. 10 (2020) 492https://doi.org/10.3390/biom10030492.
[48] M.X. Sun, F. Yu, M.L. Gong, et al., Effects of curcumin on the role of MMP-2 in endometrial cancer cell proliferation and invasion, Eur. Rev. Med. Pharmacol. Sci. 22 (2018) 5033–5041https://doi.org/10.26355/eurrev_201808_15646.
[49] M.D. Sternlicht, Z. Werb, How matrix metalloproteinases regulate cell behavior, Annu. Rev. Cell. 17 (2001) 463–516https://doi.org/10.1146/annurev.cellbio.17.1.463.
[50] [42] R.L. Daniel, M.I. Olaia, F. Catalina, et al., In vitro anti-proliferative and anti-invasive effect of polysaccharide-rich extracts from *Trametes Versicolor* and *Grifola Frondosa* in colon cancer cells, Int. J. Med. Sci. 16 (2019) 231–240http://www.medsci.org/v16p0231.htm.
[51] X.M. Li, J.H. Peng, Z.L. Sun, et al., Chinese medicine CGA formula ameliorates DMN-induced liver fibrosis in rats via inhibiting MMP2/9, TIMP1/2 and the TGF-β/Smad signaling pathways, Acta. Pharmacol. Sin. 37 (2016) 783–793https://doi.org/10.1038/aps.2016.35.
[52] S.P. Wasser, Medicinal mushroom science: current prospects, advances, evidences, and challenges [J], Biom. J. 37 (6) (2014) 345–356http://refhub.elsevier.com/S0141-8130(19)38698-2/rf0025.
[53] X.Y. Zhang, S.W. Zhao, X.B. Song, et al., Inhibition Effect of *Glycyrrhiza* Polysaccharide (GCP) on Tumor Growth Through Regulation of the Gut Microbiota Composition, J Pharmacol Sci. 137 (4) (2018) 324–332https://linkinghub.elsevier.com/retrieve/pii/S1347-8613(18)30059-8.
[54] S.H. Hwang, M.S. Shin, T.J. Yoon, et al., Immunoadjuvant activity in mice of polysaccharides isolated from the leaves of *Panax Ginseng* C.A. Meyer, Int J Biol Macromol. 107 (2018) 2695–2700https://doi.org/10.1016/j.ijbiomac.2017.10.160.
[55] S. Sun, K.J. Li, Z.F. Lei, et al., Immunomodulatory activity of polysaccharide from *Helicteres Angustifolia* L. On 4T1 tumor-bearing mice, Biomed Pharmacother. 101 (2018) 881–888https://doi.org/10.1016/j.biopha.2018.03.029.
[56] Y.J. Chang, M. Zhang, Y.F. Jiang, et al., Preclinical and Clinical Studies of *Coriolus Versicolor* Polysaccharopeptide as an Immunotherapeutic in China, Discov Med. 23 (127) (2017) 207–219.
[57] K.W. Luo, G.G.L. Yue, C.H. Ko, et al., In vivo and in vitro anti-tumor and anti-metastasis effects of Coriolus versicolor aqueous extract on mouse mammary 4T1 carcinoma, Phytomedicine 21 (8–9) (2014) 1078–1087https://linkinghub.elsevier.com/retrieve/pii/S0944-7113(14)00204-9.
[58] H. Xu, S.W. Zou, X.J. Xu, et al., Anti-tumor Effect of β-Glucan From Lentinus Edodes and the Underlying Mechanism, Sci Rep. 6 (2016) 28802https://www.ncbi.nlm.nih.gov/pmc/articles/PMC4926123/.
[59] J. Zhu, J. Xu, L.L. Jiang, et al., Improved Antitumor Activity of Cisplatin Combined With Ganoderma Lucidum Polysaccharides in U14 Cervical Carcinoma-Bearing Mice, Kaohsiung J Med Sci. 35 (4) (2019) 222–229https://doi.org/10.1002/kjm2.12020.